Low Temperature Solid-State Reactions of $(NH_4)_2[MS_4]$ (M = W, Mo) with $[Cu(CH_3CN)_4](PF_6)$ and CuBr in the Presence of Bis(diphenylphosphino)methane (dppm): Crystal Structures of $[MS_4Cu_4(dppm)_4](PF_6)_2$ (M = W, Mo), $[WS_4Cu_3(dppm)_3]X$ (X = PF_6, Br), $[Cu_3(dppm)_3Br_2]Br$, $[WS_4Cu_2(dppm)_3]$, and $[(n\text{-}Bu)_4N][WS_4Cu_3Br_2(dppm)_2]$

Jian-Ping Lang and Kazuyuki Tatsumi*

Research Center for Materials Science, and Department of Chemistry, Graduate School of Science, Nagoya University, Furo-cho, Chikusa-ku, Nagoya 464-8602, Japan

Received May 19, 1998

The solid-state reactions of $(NH_4)_2[MS_4]$ (M = W, Mo), $[Cu(CH_3CN)_4](PF_6)$, and bis(diphenylphosphino)methane (dppm) at 110 °C produced pentanuclear clusters $[MS_4Cu_4(dppm)_4](PF_6)_2$ (**1**, M = W; **2**, M = Mo), while the analogous solution reaction in CH_2Cl_2 for M = W yielded a tetranuclear cluster $[WS_4Cu_3(dppm)_3](PF_6)$ (**3**). On the other hand, the $(NH_4)_2[WS_4]$/CuBr/dppm reaction system resulted in the formation of a tetranuclear cluster $[WS_4Cu_3(dppm)_3]Br$ (**4**) either in solid at 110 °C or in CH_2Cl_2, where the solid-state reaction gave also $[Cu_3(dppm)_3Br_2]Br$ (**5**) as a side product. When the solid-state reactions between $(NH_4)_2[WS_4]$, $[Cu(CH_3CN)_4](PF_6)$ (or CuBr), and dppm were carried out under the presence of $[(n\text{-}Bu)_4N]Br$, $[WS_4Cu_2(dppm)_3]$ (**6**) and $[(n\text{-}Bu)_4N][WS_4Cu_3Br_2(dppm)_2]$ (**7**) were generated, respectively, while the corresponding solution reactions in CH_2Cl_2 gave rise to **3** and **4**. Compounds **1**−**7** were fully characterized. **1** crystallizes in the orthorhombic space group *Pnma* with $a = 37.871(6)$ Å, $b = 19.667(4)$ Å, $c = 14.836(4)$ Å, and $Z = 4$. **2** crystallizes in the orthorhombic space group *Pnma* with $a = 38.00(3)$ Å, $b = 19.65(1)$ Å, $c = 14.80(1)$ Å, and $Z = 4$. **3**·CH_2Cl_2 crystallizes in the monoclinic space group $P2_1$ with $a = 13.185(5)$ Å, $b = 17.234(6)$ Å, $c = 17.791(2)$ Å, $\beta = 90.83(4)°$, and $Z = 2$. **4**·CH_2Cl_2 crystallizes in the monoclinic space group $P2_1$ with $a = 12.94(2)$ Å, $\beta = 17.06(1)$ Å, $c = 17.875(7)$ Å, $b = 93.7(1)°$, and $Z = 2$. **5**·$2(CH_3)_2CHOH$ crystallizes in the triclinic space group $P\bar{1}$ with $a = 15.613(5)$ Å, $\beta = 18.440(6)$ Å, $c = 14.191(8)$ Å, $\alpha = 99.86(4)°$, $\beta = 104.14(4)°$, $\gamma = 86.79(3)°$, and $Z = 2$. **6**·CH_2Cl_2 crystallizes in the triclinic space group $P\bar{1}$ with $a = 14.60(3)$ Å, $b = 25.6(1)$ Å, $c = 10.98(1)$ Å, $\alpha = 92.9(3)°$, $\beta = 105.1(1)°$, $\gamma = 78.7(4)°$, and $Z = 2$. **7**·$1.5CH_2Cl_2$ crystallizes in the monoclinic space group $P2_1/n$ with $a = 10.842(3)$ Å, $b = 31.08(2)$ Å, $c = 22.713(5)$ Å, $\beta = 101.29(2)°$, and $Z = 4$.

Introduction

The chemistry of mixed-metal chalcogenide clusters composed of group 6 and group 11 elements remains attractive. This can be attributed to their possible relevance to the antagonism between copper and molybdenum causing copper deficiency in ruminants,[1] and to their potential utility as nonlinear optical materials.[2] Tetrathiomolybdate and tetrathiotungstate are classical examples of building blocks for the synthesis of transition metal sulfide clusters, and yet they are still useful in the preparation of new types of cluster compounds with various nuclearity.[1−8] While these clusters are usually prepared from standard solution reactions, we have recently developed a method based on the low-temperature solid-state reactions of $[MS_4]^{2-}$ (M = W, Mo) with copper(I) and silver(I) complexes.[9,10] Reactions of $[MS_4]^{2-}$ (M = W, Mo) with copper(I)

(1) (a) Müller, A.; Diemann, E.; Jostes, R.; Bögge, H. *Angew. Chem., Int. Ed. Engl*. **1981**, *20*, 934. (b) Mills, C. F. *Philos. Trans. R. Soc. London, Ser. B* **1979**, *288*, 51.

(2) (a) Shi, S.; Ji, W.; Tang, S.-H.; Lang, J.-P.; Xin, X.-Q. *J. Am. Chem. Soc*. **1994**, *116*, 3615. (b) Shi, S.; Ji, W.; Lang, J.-P.; Xin, X. -Q. *J. Phys. Chem*. **1994**, *98*, 3570. (c) Lang, J.-P.; Tatsumi, K.; Kawaguchi, H.; Lu, J.-M.; Ge, P.; Ji, W.; Shi, S. *Inorg. Chem*. **1996**, *35*, 7924.

(3) (a) Müller, A.; Bögge, H.; Schimanski, U. *Inorg. Chim. Acta* **1983**, *69*, 5. (b) Müller, A.; Bögge, H.; Schimanski, U.; Penk, M.; Nieradzik, K.; Dartmann, M.; Krickemeyer, E.; Schimanski, J.; Romer, C.; Romer, M.; Dornfeld, H.; Wienboker, U.; Hellmann, W.; Zimmermann, M. *Monatsh. Chem*. **1989**, *120*, 367.

(4) (a) Acott, S. R.; Garner, C. D.; Nicholson, J. R.; Clegg, W. *J. Chem. Soc., Dalton Trans*. **1983**, 713. (b) Nicholson, J. R.; Flood, A. C.; Garner, C. D.; Clegg, W. *J. Chem. Soc., Chem. Commun*. **1983**, 1179. (c) Scattergood, C. D.; Bonney, P. G.; Slater, J. M.; Garner, C. D.; Clegg, W. *J. Chem. Soc., Chem. Commun*. **1987**, 1749.

(5) (a) Sécheresse, F.; Salis, M.; C. Potvin, C.; Manoli, J. M. *Inorg. Chim. Acta* **1986**, *114*, L19. (b) Manoli, J. M.; Potvin, C.; Sécheresse, F.; Marzak, S. *Inorg. Chim. Acta* **1988**, *150*, 257. (c) Sécheresse, F.; Bernes, S.; Robert, F.; Jeannin, Y. *J. Chem. Soc., Dalton Trans*. **1991**, 2875. (d) Bernes, S.; Sécheresse, F.; Jeannin, Y. *Inorg. Chim. Acta* **1992**, *191*, 11. (e) Jeannin, Y.; Sécheresse, F.; Bernes, S.; Robert, F. *Inorg. Chim. Acta* **1992**, *198*−*200*, 493.

(6) (a) Sarkar, S.; Mishra, S. B. S. *Coord. Chem. Rev*. **1984**, *59*, 239. (b) Shibahara, T.; Akashi, H.; Kuroya, H. *J. Am. Chem. Soc*. **1988**, *110*, 3313. (c) Chan, C. K.; Guo, C. X.; Wang, R. T.; Mak. T. C. W.; Che, C. M. *J. Chem. Soc., Dalton Trans*. **1995**, 753. (d) Hou, H.-W.; Xin, X.-G.; Shi, S. *Coord. Chem. Rev*. **1996**, *153*, 25. (e) Huang, Q.; Wu, X.-T.; Wang, Q.-M.; Sheng, T.-L.; Lu, J.-X. *Inorg. Chem*. **1996**, *35*, 893. (f) Wu, D.-X.; Hong, M.-C.; Cao, R.; Liu, H.-Q. *Inorg. Chem*. **1996**, *35*, 1080. (g) Ogo, S.; Suzuki, T.; Ozawa, Y.; Isobe, K. *Inorg. Chem*. **1996**, *35*, 6093.

(7) (a) Huffman, J. C.; Roth, R. S.; Siedle, A. R. *J. Am. Chem. Soc*. **1976**, *98*, 4340. (b) Stephan, D. W.; Kinsch, E. M. *Inorg. Chim. Acta* **1985**, *96*, L87. (c) Charnock, J. M.; Bristwo, S.; Nicholson, J. R.; Garner, C. D.; Clegg, W. *J. Chem. Soc., Dalton Trans*. **1987**, 303. (d) Canales, F.; Gimeno, M. C.; Jones, P. G.; Laguna, A. *J. Chem. Soc., Dalton Trans*. **1997**, 439.

(8) (a) Lang, J.-P.; Kawaguchi, H.; Ohnishi, S.; Tatsumi, K. *J. Chem. Soc., Chem. Commun*. **1997**, 405. (b) Lang, J.-P.; Kawaguchi, H.; Tatsumi, K. *Inorg. Chem*. **1997**, *36*, 6447. (c) Lang, J.-P.; Tatsumi, K. *Inorg. Chem*. **1998**, *37*, 160. (d) Lang, J.-P.; Kawaguchi, H.; Ohnishi, S.; Tatsumi, K. *Inorg. Chim. Acta* **1998**, *283*, 136.

10.1021/ic980566c CCC: $15.00
Published on Web 11/13/1998

and silver(I) in the presence of PPh_3, both in solution[3,5e] and in the solid state,[9b] were found to generate linear, cubane-like, and face-shared double cubane-like clusters, where the phosphine usually coordinates at the coinage metals. As an outgrowth of our study on the low-temperature solid-state synthesis of W(Mo)/Cu(Ag)/S clusters, we have introduced a diphosphine ligand, dppm, anticipating formation of new cluster frameworks. Herein we report the synthesis and structural characterization of a series of heterometallic sulfide clusters stabilized by dppm ligands: two pentanuclear cationic clusters $[MS_4Cu_4(dppm)_4](PF_6)_2$ (M = W, Mo), two tetranuclear cationic clusters $[WS_4Cu_3(dppm)_3]X$ (X = PF_6, Br), a tetranuclear anionic cluster $[(n\text{-}Bu)_4N][WS_4Cu_3Br_2(dppm)_2]$, and a trinuclear neutral cluster $[WS_4Cu_2(dppm)_3]$ along with a homometallic trinuclear copper cluster $[Cu_3(dppm)_3Br_2]Br$.

Results and Discussion

Solid State Reactions at Low Temperatures. The solid-state reactions of $(NH_4)_2[MS_4]$ (M = W, Mo), $[Cu(CH_3CN)_4](PF_6)$, and dppm in the molar ratio of 1:2:4 were carried out at 110 °C in Pyrex tubes fitted with rubber septa and inlet/outlet needles. During these reactions, an argon stream was introduced into the tube via an inlet needle connected to an argon line, to remove the NH_3, H_2S, and CH_3CN gases evolved. $[Cu(CH_3CN)_4](PF_6)$ is heat-sensitive and gradually releases CH_3CN molecules when it is heated, and NH_3 and H_2S are generated by partial decomposition of $(NH_4)_2[MS_4]$. In both tungsten and molybdenum cases, the reaction mixtures gradually became molten and the reddish-yellow or red color deepened afer 12 h. The mixtures were then cooled to room temperature. After layering Et_2O onto the CH_2Cl_2 extracts of the resulting solids, the pentanuclear clusters $[MS_4Cu_4(dppm)_4](PF_6)_2$ (M = W (**1**), Mo (**2**)) were isolated as red-orange and dark-red crystals in 22% and 24% yields, respectively, as shown in Scheme 1. The dppm molecule (mp = 118−119 °C) acts not only as an auxiliary ligand for cluster formation, but also as a molten reagent, which plays an important role in overcoming the low interphase reactivity in solids.[9]

The relatively low yields of **1** and **2** may be attributed to the following two reasons. First, $(NH_4)_2[MS_4]$ is heat-sensitive, and some gradual decomposition to MS_3 and/or to other clusters, e.g. $[W_3S_9]^{2-}$, occurs during the reaction,[11] to generate NH_3 and H_2S; $[Cu(CH_3CN)_4](PF_6)$ is also subject to thermal decomposition. Second, part of the starting materials remains unreacted due to the low interphase reactivity in solids. For examole, in the synthesis of **1**, 10−15% of unreacted $(NH_4)_2[WS_4]$ was recovered from the product mixture by extracting it with water. The heating temperature also influences the yield of **1** and **2**. The yield of **1** becomes as poor as <5% when the temperature is either elevated above 125 °C or lowered below 95 °C.

When the reaction of $(NH_4)_2[WS_4]$, $[Cu(CH_3CN)_4](PF_6)$, and dppm (molar ratio = 1:2:4) was carried out in CH_2Cl_2 at room temperature, a tetranuclear complex $[WS_4Cu_3(dppm)_3](PF_6)$ (**3**) was obtained in 40% yield. Interestingly, the solution reaction

Scheme 1

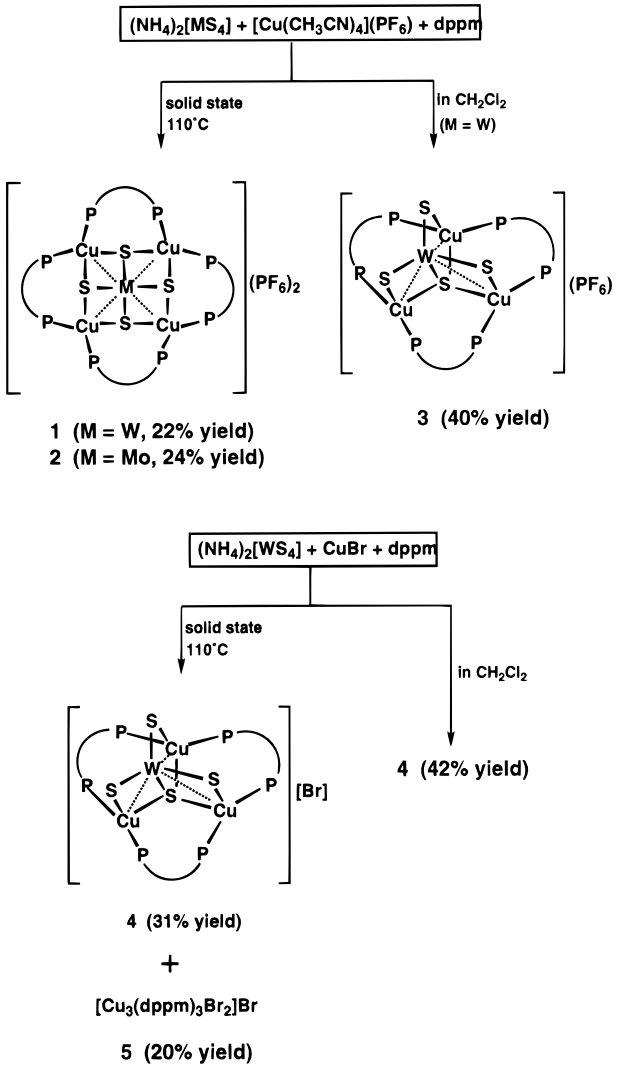

in CH_2Cl_2 did not produce the pentanuclear complex **1**, while **3** was not obtained from the corresponding solid state synthesis. The higher nuclearity of the products obtained from the low-temperature solid state reactions may be partly due to high concentrations of reactants in the molten state.

The analogous reaction with CuBr was then examined. Upon heating at 110 °C, a 1:2:4 mixture of $(NH_4)_2[WS_4]$, CuBr, and dppm gradually became sintered and its color turned from orange to lighter orange. Two products were isolated from layering Et_2O onto the CH_2Cl_2 extract of the resulting solid. One is a tetranuclear cluster $[WS_4Cu_3(dppm)_3]Br$ (**4**) and the other is a tricopper cluster $[Cu_3(dppm)_3Br_2]Br$ (**5**), obtained as orange plates (31%) and colorless prisms (20%), respectively. Treatment of the 1:2:4 $(NH_4)_2[WS_4]$/CuBr/dppm reaction system in CH_2Cl_2 at room temperature also gave rise to the tetranuclear cluster **4** in 42% yield, while the formation of **5** was not discernible in this solution reaction. Thus, with CuBr as a copper source, the solid-state and solution reactions resulted in the common WCu_3 tetranuclear cluster, while the situation contrasts to the reaction system consisting of $[Cu(CH_3CN)_4](PF_6)$, where the solid-state reaction produced the unique WCu_4 pentanuclear cluster. The disparity may arise from the different stability of the copper species at 110 °C. While CuBr is thermally stable at that temperature, $[Cu(CH_3CN)_4](PF_6)$ tends to lose CH_3CN ligands and thereby generates a reactive species in the molten state, which would promote formation of the

(9) (a) Li, J.-G.; Xin, X.-Q.; Zhou, Z.-Y.; Yu, K.-B. *J. Chem. Soc., Chem. Commun*. **1991**, 250. (b) Lang, J.-P.; Xin, X.-Q. *J. Solid State Chem*. **1994**, *108*, 118.

(10) (a) Hou, H.-W.; Xin, X.-Q.; Liu, J.; Chen, M.-Q.; Shi, S.; *J. Chem. Soc., Dalton Trans*. **1994**, 3211. (b) Shi, S.; Ji. W.; Xie, W.; Tang, S.-H.; Zeng, H. C.; Lang, J.-P.; Xin, X.-Q. *Mater. Chem. Phys*. **1995**, *39*, 298. (c) Sakane, G.; Shibahara, T.; Hou, H.-W.; Xin, X.-Q.; Shi, S. *Inorg. Chem*. **1995**, *34*, 4785. (d) Chen, Z.-R.; Hou, H.-W.; Xin, X.-Q.; Yu, K.-B. *J. Phys. Chem*. **1995**, *99*, 8717. (e) Shi, S.; Lin, Z.; Xin, X.-Q. *J. Phys. Chem*. **1996**, *100*, 10696.

(11) Koniger-Ahlborn, E.; Müller, A. *Angew. Chem., Int. Ed. Engl*. **1975**, *14*, 573.

Scheme 2

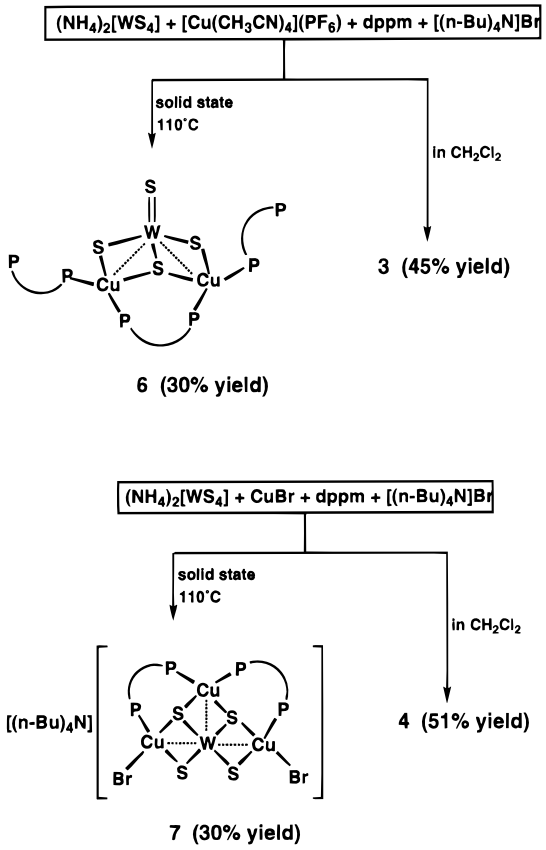

cluster with higher nuclearity. The diphosphine chelate, dppm, could be another factor favoring the WCu_4 pentanuclear structure. In fact, the solid-state reactions of $(NH_4)_2[MS_4]$ (M = Mo, W), M′X (M′ = Cu, Ag; X = Cl, Br, I) and PPh_3 were reported to give four different cluster frameworks: $[MS_4M'_2(PPh_3)_3]$ (linear structure), $[MS_4M'_3(PPh_3)_3]$ (cubane core structure), $[M'X(PPh_3)]_4$ (cubane core structure), and $[M_2S_8M'_4(PPh_3)_8]$ (face-shared double-cubane core structure).[9b]

The reactions described thus far yielded cationic clusters, and we became interested to see the effect of an ammonium salt on cluster formation. Because its relatively low melting point (103−105 °C), $[(n\text{-}Bu)_4N]Br$ is suited for low-temperature solid-state reactions. A 1:2:4:4 reaction mixture of $(NH_4)_2[WS_4]$, $[Cu(CH_3CN)_4](PF_6)$, dppm, and $[(n\text{-}Bu)_4N]Br$ was heated at 110 °C, which melted quickly; the color deepened after 12 h. A workup similar to that used for the isolation of **1** resulted in a neutral trinuclear cluster $[WS_4Cu_2(dppm)_3]$ (**6**) in 30% yield as shown in Scheme 2. This product is highly soluble in toluene, and slightly soluble in CH_3CN, whereas the complex salts **1**−**4** are insoluble in toluene. The solution reaction in CH_2Cl_2, on the other hand, gave the cationic tetranuclear cluster **3** in 45% yield, and the addition of $[(n\text{-}Bu)_4N]Br$ did not affect this solution reaction.

In the case of the (1:2:4) $(NH_4)_2[WS_4]$/CuBr/dppm, the addition of $[(n\text{-}Bu)_4N]Br$ produced an anionic WCu_3 tetranuclear cluster, $[(n\text{-}Bu)_4N][WS_4Cu_3Br_2(dppm)_2]$ (**7**) in 27% yield. In the CH_2Cl_2 solution reaction of the analogous system, again the presence of $[(n\text{-}Bu)_4N]Br$ did not alter the product, and led to the cationic cluster **4**.

Crystal Structures of $[MS_4Cu_4(dppm)_4](PF_6)_2$ (1, M = W; 2, M = Mo). Crystallized in the orthorhombic space group *Pnma*, the asymmetric unit for either **1** or **2** consists of one-half of the $[MS_4Cu_4(dppm)_4]^{2+}$ (M = W, Mo) dication and one

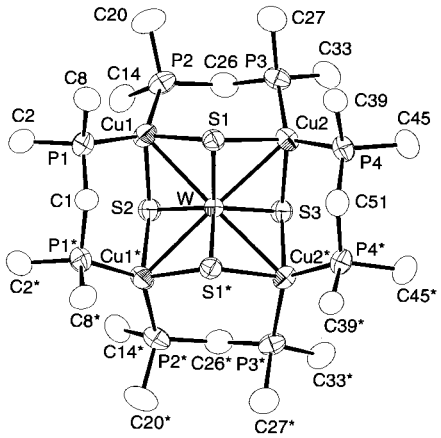

Figure 1. Structure and labeling of the $[WS_4Cu_4(dppm)_4]^{2+}$ dication of **1**. The thermal ellipsoids represent the 50% probability surfaces. All carbon atoms except for those bound to phosphorus atoms are omitted for clarity.

Table 1. Bond Lengths (Å) and Angles (deg) for $[MS_4Cu_4(dppm)_4](PF_6)_2$ (M = W (**1**), Mo, (**2**))

	1 (M = W)	**2** (M = Mo)
M−Cu(1)	2.764(1)	2.747(2)
M−Cu(2)	2.755(1)	2.737(2)
M−S(1)	2.215(2)	2.215(3)
M−S(2)	2.214(4)	2.209(4)
M−S(3)	2.219(4)	2.219(4)
Cu(1)−S(1)	2.344(3)	2.319(3)
Cu(1)−S(2)	2.361(2)	2.343(3)
Cu(2)−S(1)	2.354(3)	2.338(4)
Cu(2)−S(3)	2.345(2)	2.332(3)
Cu(1)−P(1)	2.264(3)	2.262(4)
Cu(1)−P(2)	2.273(3)	2.269(3)
Cu(2)−P(3)	2.270(3)	2.266(3)
Cu(2)−P(4)	2.268(3)	2.272(3)
Cu(1)−M−Cu(2)	89.40(4)	89.47(5)
Cu(1)−M−Cu(1*)	92.12(6)	91.84(7)
Cu(1)−M−Cu(2*)	178.47(4)	178.70(5)
Cu(2)−M−Cu(2*)	89.09(6)	89.23(7)
S(1)−M−S(1*)	107.6(1)	108.5(1)
S(1)−M−S(2)	110.10(9)	109.57(10)
S(1)−M−S(3)	110.26(8)	110.08(9)
S(2)−M−S(3)	108.5(1)	109.0(2)
S(1)−Cu(1)−S(2)	101.0(1)	101.7(1)
S(1)−Cu(1)−P(1)	101.1(1)	101.6(1)
S(1)−Cu(1)−P(2)	108.9(1)	108.6(1)
P(1)−Cu(1)−P(2)	134.7(1)	133.9(1)
S(1)−Cu(2)−S(3)	101.5(1)	102.2(1)
S(1)−Cu(2)−P(3)	104.0(1)	103.7(1)
S(1)−Cu(2)−P(4)	102.1(1)	102.0(1)
P(3)−Cu(2)−P(4)	129.9(1)	129.4(1)
Cu(1)−S(1)−Cu(2)	111.4(1)	111.9(1)
Cu(1)−S(2)−Cu(1*)	115.0(2)	114.8(2)
Cu(2)−S(3)−Cu(2*)	111.0(2)	111.0(2)

PF_6^- anion. Their cell parameters are essentially identical, as are the molecular structures of the dicationic clusters. Therefore only the perspective view of $[WS_4Cu_4(dppm)_4]^{2+}$ is shown in Figure 1, where all the phenyl groups are represented by their ipso carbons for clarity. The bond lengths and angles for **1** and **2** are compared in Table 1. The MCu_4 cluster skeleton was found in several pentanuclear M/Cu/S compounds.[4b,5a,c,6a,12−14] Table 2 compares the structural parameters of **1** and **2** with those of the known MCu_4 cluster compounds. In each of the cations,

(12) (a) Lang, J.-P.; Bian, G.-Q.; Cai, J.-H.; Kang, B.-S.; Xin, X.-Q. *Trans. Met. Chem.* **1995**, *20*, 276. (b) Lang, J.-P.; Zhou, W.-Y.; Xin, X.-Q.; Yu, K.-B. *J. Coord. Chem.* **1993**, *30*, 173.

(13) Pope, M. T.; Lang, J.-P.; Xin, X.-Q.; Yu, K.-B. *Chin. J. Chem.* **1995**, *13*, 40.

Table 2. Comparisons of Selected Bond Lengths (Å) and Angles (deg) of Pentanuclear MCu_4 Clusters (M = W, Mo)

	mean distances			mean angles		
cluster compounds	M−Cu	M−S	Cu−S	L−Cu−L	S−Cu−S	ref
$[Et_4N]_2[WS_4Cu_4(NCS)_4]$	2.691	2.221	2.297	102.9	104.4	5b
$[Et_4N]_2[MoS_4Cu_4(NCS)_4]$	2.678	2.226	2.286	102.5	105.2	5b
$[Et_4N]_4[WS_4Cu_4I_6]$	2.692	2.241	2.316	115.7	103.6	12a
$[Et_4N]_4[MoS_4Cu_4I_6]$	2.668	2.228	2.292	116.0	103.9	12b
$[WS_4Cu_4(\gamma\text{-MePy})_8][W_6O_{19}]$	2.686	2.230	2.303	108.1	104.5	13
$[WS_4Cu_4(dppm)_4](PF_6)_2$ (**1**)	2.760	2.216	2.351	132.3	101.3	this work
$[MoS_4Cu_4(dppm)_4](PF_6)_2$ (**2**)	2.742	2.214	2.333	131.7	102.0	this work

Table 3. Selected Bond Lengths (Å) and Angles (deg) for $[WS_4Cu_3(dppm)_3](PF_6)$ (**3**) and $[WS_4Cu_3(dppm)_3]Br$ (**4**)

	3	**4**		**3**	**4**
W−Cu(1)	2.789(2)	2.842(3)	W−Cu(2)	2.800(1)	2.809(3)
W−Cu(3)	2.826(2)	2.815(4)	W−S(1)	2.278(2)	2.331(6)
W−S(2)	2.202(3)	2.243(6)	W−S(3)	2.189(2)	2.194(5)
W−S(4)	2.180(3)	2.100(6)	Cu(1)−S(1)	2.323(2)	2.312(6)
Cu(1)−S(2)	2.326(3)	2.327(7)	Cu(2)−S(1)	2.316(2)	2.322(6)
Cu(2)−S(3)	2.360(3)	2.324(7)	Cu(3)−S(1)	2.318(3)	2.353(6)
Cu(3)−S(4)	2.389(3)	2.355(7)	Cu(1)−P(1)	2.291(3)	2.321(6)
Cu(1)−P(6)	2.296(3)	2.289(7)	Cu(2)−P(2)	2.284(3)	2.332(6)
Cu(2)−P(3)	2.299(3)	2.274(7)	Cu(3)−P(4)	2.280(3)	2.264(7)
Cu(3)−P(5)	2.284(2)	2.294(7)			
S(1)−W−S(2)	107.39(9)	104.8(2)	S(2)−W−S(3)	112.38(9)	111.3(2)
S(3)−W−S(4)	110.3(1)	112.3(3)	S(4)−W−S(1)	107.88(9)	108.3(2)
Cu(1)−W−Cu(2)	85.43(5)	83.94(8)	Cu(1)−W−Cu(3)	89.95(4)	89.60(9)
Cu(2)−W−Cu(3)	87.33(3)	87.61(9)	Cu(1)−S(1)−Cu(2)	109.63(9)	109.3(3)
Cu(1)−S(1)−Cu(3)	117.53(9)	117.4(2)	Cu(2)−S(1)−Cu(3)	113.94(8)	112.8(2)
W−S(1)−Cu(1)	74.62(6)	75.5(2)	W−S(1)−Cu(2)	75.12(6)	74.3(2)
W−S(1)−Cu(3)	75.87(7)	73.9(2)	W−S(2)−Cu(1)	76.00(8)	76.9(2)
W−S(3)−Cu(2)	75.91(7)	76.8(2)	W−S(4)−Cu(1)	76.25(8)	78.1(2)

the tetrahedral MS_4 (M = W, Mo) moiety is coordinated by four copper atoms, which are further bridged by four dppm molecules. A crystallographic mirror plane runs through the central metal atom, S(2), S(3), C(1), and C(51), and the pentanuclear MCu_4 cluster has an approximate D_{2h} symmetry. The four Cu atoms are crystallographically coplanar, and M sits on this plane with the very small out-of-plane displacement of 0.0002 Å for M = Mo or 0.004 Å for M = W. The structure may also be described as an MS_4 unit surrounded by a sixteen-membered [-Cu−P−C−P-]$_4$ ring. This framework resembles those of $[Cu_4(dppm)_4(CS_3)_2]$[15a] and $[Cu_4(dppm)_4E](PF_6)_2$ (E = S,[15b] Se[15c]), where two trithiocarbonate anions or an E^{2-} anion are encapsulated by a similar sixteen-membered ring.

The mean M−S lengths of **1** and **2** are somewhat shorter compared with those of the other MCu_4 clusters, yet they are understandably longer than the average M−S double bond lengths found in $(NH_4)_2[MS_4]$ (2.165 Å for M = W,[16a] 2.17 Å for M = Mo[16b]). On the other hand, Cu−S bond lengths of **1** and **2** are generally longer than in the other MCu_4 clusters. It seems that the four Cu atoms are pulled outward in order to release the strain of the [-Cu−P−C−P-]$_4$ ring caused by the steric bulk of dppm. This effect is reflected in the longer (ca. 0.04 Å) Cu−S distances and also in the elongation (ca. 0.07 Å) of the M-Cu bonds, relative to the corresponding known MCu_4 clusters. Nevertheless, the observed M−Cu distances of **1** and **2** suggest the presence of metal−metal bonds, and the acute M−S−Cu angles (74.09(8)−74.59(8)° for **1**, 73.84(9)−74.55(9)° for **2**) corroborate the argument. The tetrahedral coordination geometry of each copper atom is severely distorted, while the average Cu−P lengths are not unusual. Particularly significant are the P−Cu−P angles which are as large as 132.3° (av) for **1** and 131.7° (av) for **2**, in contrast to the small S−Cu−S angles of 101.3° (av) for **1** and 102.0° (av) for **2**. These angular distortions appear to be caused by steric bulkiness of dppm. The difference between the average P−Cu−P and S−Cu−S angles amounts to ca. 30°, and this distortion is unique among the MCu_4 cluster structures shown in Table 2. At the periphery of the cluster frames of **1** and **2**, four $\overline{\text{CuSCuPCP}}$ six-membered rings adopt a twisted chair conformation. All Cu−P−C angles, except for the Cu(1)−P(2)−C(14) and Cu(2)−P(4)−C(39) angles, are greater than 109.5°, whereas all C−P−C angles are smaller.

Crystal Structures of $[WS_4Cu_3(dppm)_3]X$ (3, X = PF_6; 4, X = Br). Having a common chemical formula $[WS_4Cu_3(dppm)_3]X$, **3** and **4** both crystallize in the monoclinic space group $P2_1$, and they are solvated by CH_2Cl_2. As the structures of the cations of **3** and **4** are very similar to that in $[WS_4Cu_3(dppm)_3](ClO_4)$,[6c] we describe only their salient geometrical features. Figure 2 shows the view of **4**, and Table 3 summarizes the selected bond lengths and angles of **3** and **4**. The cluster framework of **3** and **4** consists of a WS_4 unit coordinated by three copper atoms, forming a distorted "flywheel" array, which are bridged by three dppm ligands. Alternatively, the structure is viewed as a WS_4 unit sitting at a twelve-membered [-Cu−P−C−P-]$_3$ ring. There are two different types of sulfur atoms; one bridges W and one Cu atom, and the other is bound to W and three Cu atoms. The W−Cu lengths are slightly longer than those of **1** and **2**.

(14) (a) Jin, G.-X.; Xin, X.-Q.; Dai, A.-B.; Wang, B.; Zheng, P.-J. *Ziran Zazhi* **1987**, *10*, 873. (b) Christuk, C. C.; Ibers, J. A. *Inorg. Chem.* **1993**, *32*, 5105.

(15) (a) Lanfred, A. M. M.; Tiripicchio, A.; Camus, A.; Marsich, N. *J. Chem. Soc., Chem. Commun.* **1983**, 1126. (b) Yam, V. W. W.; Lee, W. K.; Lai, T. F. *J. Chem. Soc., Chem. Commum.* **1993**, 1571. (c) Yam, V. W. W.; Lo, K. K. W.; Cheung, K. K. *Inorg. Chem.* **1996**, *35*, 3459.

(16) (a) Sasari, K. *Acta Crystallogr. B* **1963**, *16*, 719. (b) Schäfer, H.; Schäfer, G.; Weiss, A. *Z. Naturforsch., B: Anorg. Chem., Org. Chem., Biochem., Biophys. Biol.* **1964**, *19B*, 76.

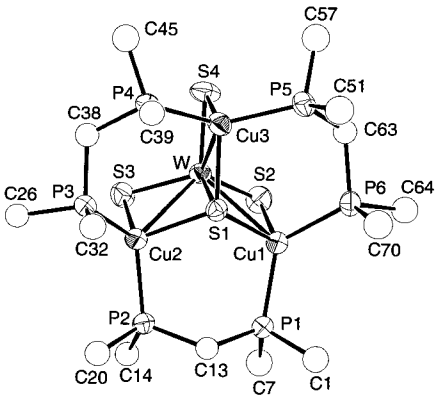

Figure 2. Structure and labeling of the $[WS_4Cu_3(dppm)_3]^+$ cation of **4**. Thermal ellipsoids are drawn at the 50% probability level. All phenyl groups are represented by their ipso carbon atoms for clarity.

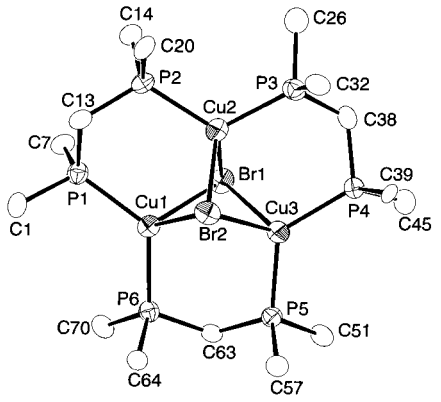

Figure 3. Structure and labeling of the $[Cu_3(dppm)_3Br_2]^+$ cation of **5**. Thermal ellipsoids are drawn at the 50% probability level. All phenyl groups are represented by their ipso carbon atoms for clarity.

Table 4. Selected Bond Lengths (Å) and Angles (deg) for $[Cu_3(dppm)_3Br_2]Br$ (**5**)

Br(1)−Cu(1)	2.625(2)	Br(1)−Cu(2)	2.628(2)
Br(1)−Cu(3)	2.550(2)	Br(2)−Cu(1)	2.591(2)
Br(2)−Cu(2)	2.518(2)	Br2−Cu(3)	2.674(2)
Cu(1)−P(1)	2.264(4)	Cu(1)−P(6)	2.265(3)
Cu(2)−P(2)	2.241(3)	Cu(2)−P(3)	2.245(3)
Cu(3)−P(4)	2.246(3)	Cu(3)−P(5)	2.251(3)
Cu(1)−Br(1)−Cu(2)	73.01(5)	Cu(1)−Br(1)−Cu(3)	78.67(6)
Cu(2)−Br(1)−Cu(3)	74.49(6)	Cu(1)−Br(2)−Cu(2)	75.41(6)
Cu(1)−Br(2)−Cu(3)	77.08(6)	Cu(2)−Br(2)−Cu(3)	74.21(6)
Br(1)−Cu(1)−Br(2)	89.59(6)	Br(1)−Cu(1)−P(1)	106.57(10)
Br(1)−Cu(1)−P(6)	106.19(9)	P(1)−Cu(1)−P(6)	125.9(1)
Br(1)−Cu(2)−Br(2)	91.13(6)	Br(1)−Cu(2)−P(2)	114.4(1)
Br(1)−Cu(2)−P(3)	108.1(1)	P(2)−Cu(2)−P(3)	117.5(1)
Br(1)−Cu(3)−Br(2)	89.40(7)	Br(1)−Cu(3)−P(4)	105.8(1)
Br(1)−Cu(3)−P(5)	107.7(1)	P(4)−Cu(3)−P(5)	124.8(1)

Crystal Structure of $[Cu_3(dppm)_3Br_2]Br$ (5). An asymmetric unit of the crystals of **5** contains one $[Cu_3(dppm)_3Br_2]^+$ cation, one Br^- anion, and two 2-propanol solvent molecules. The structure of the cation is shown in Figure 3, and the selected bond lengths and angles are given in Table 4. The structure of the chloride analogue of **5** has been reported.[17] The trigonal-prismatic Cu_3Br_2 core is coordinated by three dppm ligands. The tetrahedral coordination geometry of each copper is distorted with a large P−Cu−P and a small Br−Cu−Br angle. An interesting geometrical feature of **5** is that Br(1) caps copper atoms with one short (2.550(2) Å) and two long (2.625(2) Å and 2.628(2) Å) bonds, whereas coordination of Br(2) occurs with two short (2.518(2) Å and 2.591(2) Å) and one long (2.674(2) Å) bonds. This asymmetric capping mode may be induced by the steric bulk of the phenyl groups of dppm.

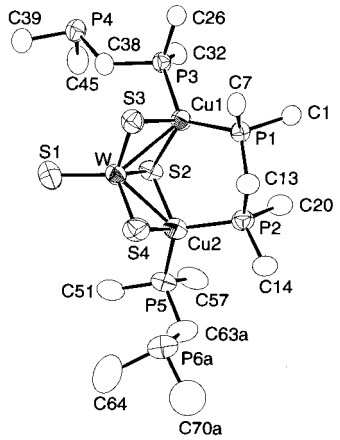

Figure 4. Molecular structure and labeling of $[WS_4Cu_2(dppm)_3]$ (**6**), where only one set of the disordered P(6) and C(63) atoms and the disordered phenyl group is shown. Thermal ellipsoids are drawn at the 50% probability level. All phenyl groups are represented by their ipso carbon atoms for clarity.

Table 5. Selected Bond Lengths (Å) and Angles (deg) for $[WS_4Cu_2(dppm)_3]$ (**6**)

W−Cu(1)	2.836(1)	W−Cu(2)	2.7914(9)
W−S(1)	2.146(4)	W−S(2)	2.256(1)
W−S(3)	2.177(1)	W−S(4)	2.206(2)
Cu(1)−S(2)	2.331(2)	Cu(1)−S(3)	2.392(1)
Cu(2)−S(2)	2.320(2)	Cu(2)−S(4)	2.337(1)
Cu(1)−P(1)	2.282(4)	Cu(1)−P(3)	2.259(2)
Cu(2)−P(2)	2.285(4)	Cu(2)−P(5)	2.255(2)
S(1)−W−S(2)	110.36(6)	S(1)−W−S(3)	110.92(8)
S(1)−W−S(4)	111.81(8)	S(3)−W−S(4)	109.77(9)
Cu(1)−W−Cu(2)	80.00(4)	Cu(1)−S(2)−Cu(2)	102.13(10)
S(2)−Cu(1)−S(3)	98.11(4)	S(2)−Cu(1)−P(1)	121.04(8)
S(3)−Cu(1)−P(3)	100.90(4)	P(1)−Cu(1)−P(3)	128.13(5)
S(2)−Cu(2)−S(4)	101.38(4)	S(2)−Cu(2)−P(2)	109.94(8)
S(4)−Cu(2)−P(5)	114.38(5)	P(2)−Cu(2)−P(5)	114.53(7)
W−S(2)−Cu(1)	76.38(3)	W−S(2)−Cu(2)	75.15(3)
W−S(3)−Cu(1)	76.59(4)	W−S(4)−Cu(2)	75.76(3)

Crystal Structure of $[WS_4Cu_2(dppm)_3]$ (6). The crystals of **6** are solvated by 1 equiv of CH_2Cl_2 molecules. The molecular view and the structure parameters are presented in Figure 4 and in Table 5. The WS_4Cu_2 core structure resembles the $MOS_3M'_2$ moieties found in $[MOS_3M'_2(PPh_3)_3]$ (M = W, Mo; M′ = Cu(I), Ag(I)),[18] $[MoOS_3(CuSPh)_2]^{2-}$,[19] and $[MoOS_3Cu_2(PPh_3)_2(Py)_2]$.[20] However, coordination of two coinage metal atoms to tetrathiometalate, leaving one M=S bond intact, is rare, and $[ReS_4(CuNCS)_2]^-$ is the sole example of such a type.[24a] The average W−μ_2-S bond length is 0.05 Å longer

(17) Bersciani, N.; Marsich, N.; Nardin, G.; Randaccio, L. *Inorg. Chim. Acta* **1974**, *10*, L5.

(18) (a) Müller, A.; Bögge, H.; Schimanski, J. *Inorg. Chim. Acta* **1983**, *76*, L245. (b) Du, S.-W.; Zhu, N.-Y.; Chen, P.-C.; Wu, X.-T. *Polyhedron* **1992**, *19*, 2489.

(19) Müller, A.; Dartmann, M.; Römer, C.; Clegg, W.; Sheldrick, G. M. *Angew. Chem., Int. Ed. Engl*. **1981**, *20*, 1060.

(20) Hou, H.-W.; Xin, X.-Q.; Huang, X.-Y.; Cai, J.-H.; Kang, B.-S. *Chin. Chem. Lett*. **1995**, *6*, 91.

(21) Müller, A.; Krickemeyer, E.; Hildebrand, A.; Bögge, H.; Schneider, K.; Lemke, M. *J. Chem. Soc., Chem. Commun*. **1991**, 1685.

(22) (a) Manoli, J. M.; Potvin, C.; Sécheresse, F. *J. Chem. Soc., Chem. Chmmun*. **1982**, 1159. (b) Minelli, M.; Enemark, J. H.; Nicholson, J. R.; Garner, C. D. *Inorg. Chem*. **1984**, *23*, 4384.

(23) (a) Müller, A.; Schimanski, J.; Bögge, H. *Z. Anorg. All. Chem*. **1987**, *544*, 107. (b) Manoli, J. M.; Potvin, C.; Sécheresse, F.; Marzak, S. *Inorg. Chim. Acta* **1988**, *150*, 257.

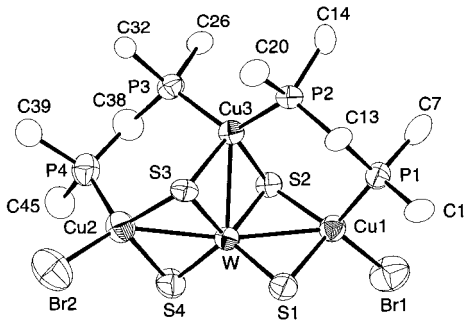

Figure 5. Structure and labeling of $[WS_4Cu_3Br_2(dppm)_2]^-$ anion of **7**. Thermal ellipsoids are drawn at the 50% probability level. All phenyl groups are represented by their ipso carbon atoms for clarity.

Table 6. Selected Bond Lengths (Å) and Angles (deg) for $[(n\text{-}Bu)_4N][WS_4Cu_3Br_2(dppm)_2]$ (**7**)

W−Cu(1)	2.748(3)	W−Cu(2)	2.765(3)
W−Cu(3)	2.807(3)	W−S(1)	2.185(5)
W−S(2)	2.244(5)	W−S(3)	2.242(5)
W−S(4)	2.171(6)	Br(1)−Cu(1)	2.405(4)
Br(2)−Cu(2)	2.380(4)	Cu(1)−S(1)	2.339(6)
Cu(1)−S(2)	2.308(6)	Cu(2)−S(3)	2.344(7)
Cu(2)−S(4)	2.329(7)	Cu(3)−S(2)	2.331(6)
Cu(3)−S(3)	2.336(5)	Cu(1)−P(1)	2.283(6)
Cu(2)−P(4)	2.292(7)	Cu(3)−P(2)	2.287(6)
Cu(3)−P(3)	2.289(6)		
Cu(1)−W−Cu(2)	168.06(8)	Cu(1)−W−Cu(3)	82.85(7)
Cu(2)−W−Cu(3)	85.59(7)	S(1)−W−S(2)	108.9(2)
S(1)−W−S(3)	110.2(2)	S(1)−W−S(4)	111.9(2)
S(2)−W−S(4)	109.9(2)	S(1)−Cu(1)−S(2)	101.7(2)
S(3)−Cu(2)−S(4)	100.3(2)	S(2)−Cu(3)−S(3)	101.3(2)
W−S(1)−Cu(1)	74.7(2)	W−S(2)−Cu(1)	74.3(2)
W−S(2)−Cu(3)	75.7(2)	W−S(3)−Cu(2)	74.1(2)
W−S(3)−Cu(3)	75.6(2)	W−S(4)−Cu(2)	75.7(2)

than the W═S(1) bond, but it is 0.06 Å shorter than the W−μ_3-S(2) bond. The two planar WS_2Cu rhombs are folded with a dihedral angle of 69°. The mean W−Cu length (2.815 Å) is 0.06 Å longer than that of **1** and close to those of **3** and **4**. One of the three dppm ligands bridges the two copper sites, and the other two are monodentate. Due to the dppm bridge, the Cu(1)−W−Cu(2) bond angle is ca. 10° smaller than that observed in $[MOS_3M'_2(PPh_3)_3]$ (M = W, Mo; M′ = Cu(I), Ag(I)), $[MoOS_3(CuSPh)_2]^{2-}$, and $[MoOS_3Cu_2(PPh_3)_2(Py)_2]$. Occurrence of this η^1-coordination of dppm is uncommon. As discussed later in Concluding Remarks, an alternation coordination mode of dppm at the WS_4Cu_2 core could be that one dppm ligand chelates at each copper atom with the formula $WS_4Cu_2(dppm)_2$. This geometry does not invoke the unusual η^1-coordination of dppm, but it may introduce a steric problem between phenyl groups.

Crystal Structure of $[(n\text{-}Bu)_4N][WS_4Cu_3Br_2(dppm)_2]$ (7). The complex salt of **7** crystallizes with 1.5 equiv of CH_2Cl_2 solvent molecules. Figure 5 shows the X-ray derived structure of the complex anion, and Table 6 gives the selected bond lengths and angles. Three Cu atoms are bound to a tetrahedral WS_4 unit at three S−S edges, which are further coordinated by two dppm bridges. Thus two of the four S atoms are doubly bridging metal atoms, and the other two are triply bridging. The WCu_3 skeleton is approximately T-shaped with the Cu(1)−W−Cu(2) angle of 168.06(8)°. The W−Cu(3) distance is slightly longer than the other two W−Cu distances, while the average W−Cu length (2.773 Å) is close to that observed in **1**. This WS_4Cu_3 core structure is similar to those of $[MS_4(CuX)_3]^{2-}$ (M═Mo,W; X═Cl,Br,I),[22] $[VS_4Cu_3(PPh_3)_4]$,[23a] $[WS_4(CuNCS)_3]^{2-}$,[23b] and $[MS_4Cu_3(C_5H_{10}dtc)_3]^{2-}$.[24]

Spectral Features. The IR spectra of **1**−**4**, **6**, and **7** show two bands assignable to W−S−Cu or Mo−S−Cu stretching vibrations in the 417−451 and 470−480 cm^{-1} regions. Unique among these spectra is the presence of a W═S stretching band at 505 cm^{-1} for **6**. For **1**, **2**, and **3**, strong peaks arising from PF_6 also appear at 838 (or 840) and 557 cm^{-1}.

The ^1H NMR spectra in CD_2Cl_2 at room temperature show the correct aromatic/ methylene proton ratios of dppm for **1**−**7**. For **1**−**3**, the methylene protons split into two doublets of multiplets, indicating that two methylene protons of each dppm ligand are inequivalent. The chair conformation of $\overline{CuSCuPCP}$ rings of **1** and **2** appear to be rigid even in solution, while in the case of **3**, it is obvious from the X-ray structure that the chemical environment of two protons of dppm are different. For **4**−**7**, both the aromatic protons and methylene protons appeared as very sharp singlets. It seems that the dppm ligands in these complexes exchange their coordination sites in CD_2Cl_2 at the NMR time scale and/or that the exchange occurs between dppm and bromide.[25] The $^{31}P\{^1H\}$ NMR spectra of **1**−**3** in CD_2Cl_2 exhibited ^{31}P signals of both dppm and PF_6. The ^{31}P signals of dppm in **1**−**3** and **5** are slightly broad, partly due to the coupling between the ^{63}Cu (^{65}Cu) and ^{31}P nuclei. On the other hand, the $^{31}P\{^1H\}$ NMR signals of **4**, **6**, and **7** are much broader, which may be ascribed to possible ligand exchange process in addition to the ^{63}Cu (^{65}Cu)/^{31}P coupling.

The electronic spectra of **1**−**4** are characterized by three absorptions in the 317−572 nm range, while there appear two absorptions in the spectra of **6** and **7**. Comparison of the spectra of **1** and **2** indicates that the three absorption bands of **1** at 323, 386, and 476 nm are red-shifted to 356, 436, and 572 nm, respectively, in the spectrum of **2**. The bathochromic shifts, amounting to 0.36, 0.37, and 0.44 eV, are most likely to arise from the lower positioning of vacant 4d orbital levels of Mo relative to 5d levels of W. Similar bathochromic shifts were observed in going from $[MoS_4]^{2-}$ to $[WS_4]^{2-}$ [26] and from $[(\eta^5\text{-}C_5Me_5)MoS_3]^-$ to $[(\eta^5\text{-}C_5Me_5)WS_3]^-$.[27] Thus, the absorptions in the spectra of **1**−**4**, **6**, and **7** are probably dominated by the internal S-to-M (M = W, Mo) charge-transfer transitions of the $[MS_4]^{2-}$ moieties.[26]

Concluding Remarks

We have demonstrated that the low-temperature solid-state reactions of $(NH_4)_2[MS_4]$ (M = W, Mo) with either $[Cu(CH_3CN)_4](PF_6)$ or CuBr in the presence of dppm produced a series of M/Cu/S/dppm cluster complexes. Except for the $(NH_4)_2[WS_4]$/CuBr/dppm reaction system, the solid-state syntheses gave rise to clusters which are different from the products of the corresponding solution synthesis in CH_2Cl_2. These dppm-containing clusters may exhibit interesting photophysical properties.[6c] In fact, a preliminary investigation shows that **1**

(24) Huang, Z.-Y.; Lei, X.-J.; Liu, J.-N.; Kang, B.-S.; Liu, Q.-T.; Hong, M.-C.; Liu, H.-Q. *Inorg. Chim. Acta* **1990**, *165*, 25.

(25) (a) Berners-Price, S. J.; Johnson, R. K.; Mirabelli, C. K.; Faucetti, L. F.; McCabe, F. L.; Sadler, P. J. *Inorg. Chem.* **1987**, *26*, 3383. (b) Lewis, J. S.; Zweit, J.; Blower, P. J. *Polyhedron* **1998**, *17*, 513.

(26) (a) Gheller, S. F.; Hambley, T. W.; Rodgers, J. R.; Brownlee, R. T. C.; O'Connor, M. J.; Snow, M. R.; Wedd, A. G., *Inorg. Chem.* **1984**, *23*, 2519. (b) McDonald, J. W.; Friesen, G. D.; Rosenhein, L. D.; Newton, W. E. *Inorg. Chim. Acta* **1983**, *72*, 205. (c) Sécheresse, F.; Robert, F.; Marzak, S.; Manoli, J. M.; Potvin, C. *Inorg. Chim. Acta* **1991**, *182*, 221.

(27) (a) Kawaguchi, H.; Tatsumi, K. *J. Am. Chem. Soc.* **1995**, *117*, 3885. (b) Kawaguchi, H.; Yamada, K.; Lang, J.-P.; Tatsumi, K. *J. Am. Chem. Soc.* **1997**, *119*, 10346.

Chart 1

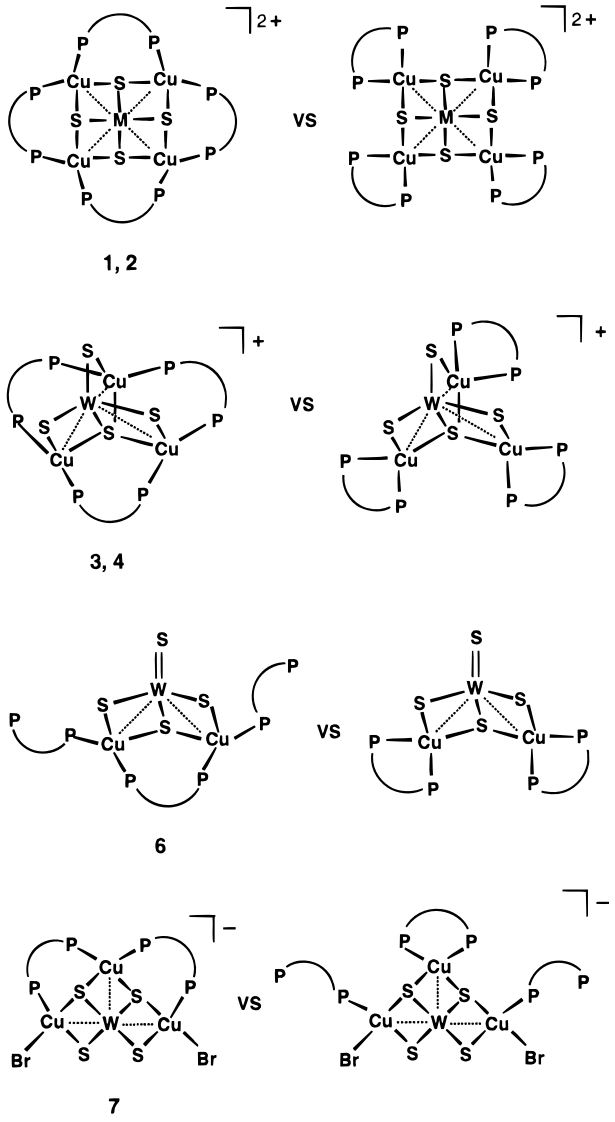

has third-order nonlinear optical properties.[28] It is expected that solid-state reactions of $[MS_4]^{2-}$ (M = W, Mo) and copper(I) with other diphosphine ligands such as dppe (1,2-bis(diphenylphosphino)ethane) will produce another series of intriguing W(Mo)/Cu/S clusters.

Having a set of M/Cu/S dppm clusters in hand, it is of interest to consider the role of dppm in stabilizing the observed cluster structures. In this light, we show in Chart 1 a possible alternative geometry of each cluster framework, where chelation of dppm at a single Cu center is emphasized. It is obvious from the observed structures that dppm has tendency to bridge two Cu atoms, probably due to the steric bulk of the phenyl groups. However, the alternative structures shown in Chart 1 are electronically feasible, and some of them could be isolated and/or could exist as intermediates of polytopal rearrangements of dppm around the cluster cores.

Experimental Section

General Procedures. All the solid-state reactions were carried out under argon atmosphere. $(NH_4)_2[MoS_4]$[26b] and $[Cu(CH_3CN)_4](PF_6)$[29] were prepared as reported in the literature, while $(NH_4)_2[WS_4]$ and other chemicals were obtained from commercial sources and were used as received. All solvents were predried over activated molecular sieves and refluxed over the appropriate drying reagents under argon and collected by distillation. FT-IR spectra in the 400−4000 cm^{-1} range were recorded on a Perkin-Elmer FT-IR 2000 spectrophotometer using KBr pellets. UV−vis spectra were measured on a JASCO V560 spectrophotometer. ^1H and $^{31}P\{^1H\}$ NMR spectra were recorded on a Varian UNITYplus-500 spectrometer at ambient temperature. ^1H NMR chemical shifts are reported relative to undeutetrated impurities of CD_2Cl_2. $^{31}P\{^1H\}$ NMR chemical shifts are referenced to the ^{31}P signal of 85% H_3PO_4 as the external standard. Elemental analyses were carried out on a LECO CHNS-932 elemental analyzer. Prior to the ^1H and $^{31}P\{^1H\}$ NMR measurements and elemental analysis, samples were dried in vacuo.

Preparation of $[WS_4Cu_4(dppm)_4](PF_6)_2$ (1). A well-ground mixture of $(NH_4)_2[WS_4]$ (0.18 g, 0.5 mmol), $[Cu(CH_3CN)_4](PF_6)$ (0.37 g, 1.0 mmol), and dppm (0.77 g, 2.0 mmol) was placed in an open Pyrex glass tube and then heated at 110 °C for 12 h. During this time, the mixture gradually melted and its color turned from orange to red-orange. After the molten mixture was allowed to cool to room temperature, it was extracted with CH_2Cl_2 (20 mL), and filtered. Red-orange crystals of **1** were isolated by layering Et_2O (20 mL) onto the filtrate for 5 days. The crystals were then collected by filtration and washed with CH_2Cl_2/Et_2O (1:4) and dried in vacuo. Yield: 0.13 g (22%). Anal. Calcd for $C_{100}H_{88}Cu_4F_{12}P_{10}S_4W$: C, 50.2; H, 3.7; S, 5.4. Found: C, 49.9; H, 3.6; S, 5.5. UV−vis (CH_2Cl_2) (λ_{max}/nm (ϵ/M^{-1} cm^{-1})): 323 (14 800), 386 (7000), 476 (2900). IR (KBr disk): 1483 (s), 1473 (s), 1363 (w), 1307 (w), 1101 (s), 1000 (m), 838 (vs), 771 (s), 737 (s), 691 (s), 557 (s), 516 (s), 478 (m), 451 (m) cm^{-1}. ^1H NMR (CD_2Cl_2, 500 MHz): δ 7.01−7.47 (m, 80H, PPh_2), 3.17 (dm, $^1J_{HH}$ = 13.5 Hz, 4H, CH_2), 2.83 (dm, $^1J_{HH}$ = 13.5 Hz, 4H, CH_2). $^{31}P\{^1H\}$ NMR (CD_2Cl_2): δ −8.42 (br s, dppm, $w_{1/2}$ = 30.3 Hz), −144.0 (h, PF_6)

Preparation of $[MoS_4Cu_4(dppm)_4](PF_6)_2$ (2). The analogous molybdenum compound **2** was prepared as above starting from $(NH_4)_2[MoS_4]$ (0.13 g, 0.5 mmol), $[Cu(CH_3CN)_4](PF_6)$ (0.37 g, 1.0 mmol), and dppm (0.77 g, 2.0 mmol). During the reaction, the mixture gradually melted and its color turned from red to dark red. Yield: 0.14 g (24%). Anal. Calcd for $C_{100}H_{88}Cu_4F_{12}MoP_{10}S_4$: C, 52.1; H, 3.9; S, 5.6. Found: C, 51.8; H, 3.8; S, 5.8. UV−vis (CH_2Cl_2) (λ_{max}/nm (ϵ/M^{-1} cm^{-1})): 356 (16 100), 436 (10 400), 572 (4400). IR (KBr disk): 1484 (s), 1436 (s), 1363 (w), 1309 (w), 1098 (s), 1000 (m), 838 (vs), 771 (s), 738 (s), 691 (s), 557 (s), 512 (s), 479 (s), 439 (m) cm^{-1}. ^1H NMR (CD_2Cl_2, 500 MHz): δ 6.56−7.58 (m, 80H, PPh_2), 3.26 (dm, $^1J_{HH}$ = 13.5 Hz, 4H, CH_2), 3.07 (dm, $^1J_{HH}$ = 13.5 Hz, 4H, CH_2). $^{31}P\{^1H\}$ NMR (CD_2Cl_2): δ −8.14 (br s, dppm, $w_{1/2}$ = 39.0 Hz), −144.0 (h, PF_6).

Preparation of $[WS_4Cu_3(dppm)_3](PF_6)$ (3). A mixture of $(NH_4)_2[WS_4]$ (0.18 g, 0.5 mmol), $[Cu(CH_3CN)_4](PF_6)$ (0.37 g, 1.0 mmol), and dppm (0.77 g, 2.0 mmol) in CH_2Cl_2 (40 mL) was stirred in air at ambient temperature for 14 h. The volume of the solution was reduced to 5 mL and filtered. An air stable orange crystalline solid of **3** was isolated by layering diethyl ether (5 mL) onto the CH_2Cl_2 filtrate for 3 days, which were collected by filtration and washed with CH_2Cl_2/Et_2O (1:4) and dried *in vacuo*. Yield: 0.24 g (40%). Anal. Calcd for $C_{75}H_{66}Cu_3F_6P_7S_4W$: C, 44.8; H, 3.3; S, 6.4. Found: C, 44.4; H, 3.3; S, 6.2. UV−vis (CH_2Cl_2) (λ_{max}/nm (ϵ/M^{-1} cm^{-1})): 318 (15 900), 370 (8300), 467 (2600). IR (KBr disk): 1484 (s), 1435 (s), 1364 (w), 1308 (w), 1096 (s), 1000 (w), 840 (vs), 776 (s), 741 (s), 692 (s), 557 (s), 514 (s), 470 (s), 418 (w) cm^{-1}. ^1H NMR (CD_2Cl_2, 500 MHz): δ 7.01−7.47 (m, 60H, PPh_2), 3.17 (dm, $^1J_{HH}$ = 13.5 Hz, 3H, CH_2), 2.83 (dm, $^1J_{HH}$ = 13.5 Hz, 3H, CH_2). $^{31}P\{^1H\}$ NMR (CD_2Cl_2): δ −8.39 (br s, $w_{1/2}$ = 35.1 Hz), −144.0 (h, PF_6).

The similar reaction of $(NH_4)_2[WS_4]$ (0.18 g, 0.5 mmol), $[Cu(CH_3CN)_4](PF_6)$ (0.37 g, 1.0 mmol), dppm (0.77 g, 2.0 mmol), and $[(n\text{-}Bu)_4N]Br$ (0.64 g, 2.0 mmol) in CH_2Cl_2 afforded **3** in 45% yield.

Preparation of $[WS_4Cu_3(dppm)_3]Br$ (4) and $[Cu_3(dppm)_3Br_2]Br$ (5). These two compound was prepared in a manner similar to that described for **1**, using CuBr (0.14 g, 1.0 mmol) as starting material. During this reaction, the orange mixture gradually became lighter orange and sintered. After extraction the solid with CH_2Cl_2 (20 mL) and subsequent filtration, two products were isolated from layering Et_2O

(28) Lang, J.-P.; Tatsumi, K. Unpublished results.
(29) Kubas, G. J. *Inorg. Synth*. **1990**, *28*, 68.

(20 mL) onto the filtrate for 1 week: orange-yellow needle crystals of **4** (yield: 0.18 g, 31%) and colorless crystals of **5** (yield: 0.11 g, 20%). Anal. Calcd for $C_{75}H_{66}BrCu_3P_6S_4W$ (**4**): C, 51.9; H, 3.8; S, 7.4. Found: C, 51.7; H, 3.7; S, 6.9. UV−vis (CH_2Cl_2) (λ_{max}/nm (ϵ/M^{-1} cm^{-1})): 317 (11 400), 370 (5300), 467 (1800). IR (KBr disk): 1483 (m), 1435 (s), 1364 (w), 1096 (m), 772 (m), 740 (s), 692 (s), 514 (m), 470 (s), 418(w) cm^{-1}. ^1H NMR (CD_2Cl_2, 500 MHz): δ 7.30 (br s, 60H, PPh_2), 2.83 (br s, 6H, CH_2). $^{31}P\{^1H\}$ NMR (CD_2Cl_2): δ −8.41 (br s, $w_{1/2}$ = 104.4 Hz). Anal. Calcd for $C_{75}H_{66}Br_3Cu_3P_6$ (**5**): C, 56.9; H, 4.2. Found: C, 56.7; H, 4.4. IR (KBr disk): 1483 (m), 1435 (s), 1362 (m), 1308 (w), 1098 (s), 1027 (m), 999 (m), 774 (s), 738 (s), 717 (s), 691 (s), 515 (s). ^1H NMR (CD_2Cl_2, 500 MHz): δ 7.15 (br s, 60H, PPh_2), 2.82 (br s, 6H, CH_2). $^{31}P\{^1H\}$ NMR (CD_2Cl_2): δ −16.4 (br s, $w_{1/2}$ = 48.4 Hz).

Compound **4** was also isolated in 42% yield from the reaction of $(NH_4)_2[WS_4]$, CuBr, and dppm (1:2:4) in CH_2Cl_2. The trinuclear copper complex **5** was directly obtained in 47% yield from the solid-state reaction of CuBr (0.14 g, 1.0 mmol) and dppm (0.77 g, 2.0 mmol) at 120 °C for 12 h. The crystal of **5**·2$(CH_3)_2$CHOH, which was used for the X-ray analysis, was grown from CH_2Cl_2/2-propanol.

Preparation of $[WS_4Cu_2(dppm)_3]$ (6). Compound **6** was prepared as above starting from $(NH_4)_2[WS_4]$ (0.18 g, 0.5 mmol), $[Cu(CH_3CN)_4](PF_6)$ (0.37 g, 1.0 mmol), dppm (0.77 g, 2.0 mmol), and $[(n\text{-}Bu)_4N]Br$ (0.64 g, 2.0 mmol). During the reaction, the orange mixture became molten and its color turned to lighter orange. A workup similar to that used for isolation of **1** generated yellow plates of **6**·0.5CH_2Cl_2, which were collected by filtration, washed with CH_2Cl_2/Et_2O (1:4), and dried in vacuo. Yield: 16 g (30%). Anal. Calcd for $C_{75}H_{66}Cu_2P_6S_4W$: C, 56.6; H, 4.2; S, 8.1. Found: C, 56.9; H, 4.3; S, 7.4. UV−vis (CH_2Cl_2) (λ_{max}/nm (ϵ/M^{-1} cm^{-1})): 382 (5500), 450 (2400). IR (KBr disk): 1481 (s), 1435 (s), 1156 (w), 1096 (s), 1026 (m), 999 (m), 780 (m), 736 (s), 696 (s), 505 (s), 480 (s), 449 (s) cm^{-1}. ^1H NMR (CD_2Cl_2, 500 MHz): δ 7.20 (br s, 60H, PPh_2), 2.85 (br s, 6H, CH_2). $^{31}P\{^1H\}$ NMR (CD_2Cl_2): δ −8.18 (br s, $w_{1/2}$ = 95.6 Hz), −14.23 (br s, $w_{1/2}$ = 303.7 Hz), −25.72 (br s, $w_{1/2}$ = 223.0 Hz).

Preparation of $[(n\text{-}Bu)_4N][WS_4Cu_3Br_2(dppm)_2]$ (7). Compound **7** was prepared as above starting from $(NH_4)_2[WS_4]$ (0.18 g, 0.5 mmol), CuBr (0.14 g, 1.0 mmol), dppm (0.77 g, 1.0 mmol), and $[(n\text{-}Bu)_4N]Br$ (0.64 g, 1.0 mmol). During the reaction, the orange mixture became molten and its color turned to red. Extraction of the resulting solid with CH_2Cl_2 and the subsequent procedure similar to that used for **1** afforded red prisms of **7**·1.5CH_2Cl_2, which were collected by filtration and washed with CH_2Cl_2/Et_2O (1:4) and dried in vacuo. Yield: 0.15 g (27%). Anal. Calcd for $C_{66}H_{80}Br_2Cu_3NP_4S_4W$: C, 47.4; H, 4.8; S, 7.7. Found: C, 47.8; H, 4.7; S, 7.0. UV−vis (CH_2Cl_2) (λ_{max}/nm (ϵ/M^{-1} cm^{-1})): 390 (3800), 437 (970). IR (KBr disk): 1483 (s), 1435 (s), 1097 (s), 1027 (m), 999 (m), 778 (s), 736 (s), 692 (s), 515 (s), 473 (s), 424 (m) cm^{-1}. ^1H NMR (CD_2Cl_2, 500 MHz): δ 7.29 (br s, 40H, PPh_2), 3.30 (t, 8H, $NCH_2CH_2CH_2CH_3$), 2.88 (br s, 4H, PCH_2P), 1.69 (m, 8H, $NCH_2CH_2CH_2CH_3$), 1.46 (m, 8H, $NCH_2CH_2CH_2CH_3$), 1.03 (t, 12H, $NCH_2CH_2CH_2CH_3$). $^{31}P\{^1H\}$ NMR (CD_2Cl_2): δ −10.46 (br s, $w_{1/2}$ = 84.3 Hz), −23.89 (br s, $w_{1/2}$ = 58.7 Hz). The similar reaction of $(NH_4)_2[WS_4]$ (0.18 g, 0.5 mmol), CuBr (0.14 g, 1.0 mmol), dppm (0.77 g, 1.0 mmol), and $[(n\text{-}Bu)_4N]Br$ (0.64 g, 2.0 mmol) in CH_2Cl_2 gave rise to **4** in 51% yield.

X-ray Crystallography. All measurements were made on a Rigaku AFC7R diffractometer at ambient temperature by using monochromated Mo Kα radiation (λ = 0.710 69 Å). A red-orange crystal of **1** with dimensions 0.90 × 0.35 × 0.40 mm, a dark red crystal of **2** with dimensions 0.45 × 0.40 × 0.80 mm, an orange crystal of **3**·CH_2Cl_2 with dimensions 0.60 × 0.45 × 0.20 mm, an orange crystal of **4**·CH_2Cl_2 with dimensions 0.40 × 0.55 × 0.45 mm, a yellow crystal of **6**·CH_2Cl_2 with dimensions 0.20 × 0.25 × 0.30 mm, and a red crystal of **7**·1.5CH_2Cl_2 with dimensions 0.60 × 0.30 × 0.25 mm, were sealed in glass capillaries, all of which were grown from CH_2Cl_2/Et_2O. A colorless prismatic crystal of **5**·2$(CH_3)_2$CHOH with dimensions 0.70 × 0.45 × 0.25 mm obtained from CH_2Cl_2/2-propanol was mounted at the top of a glass fiber. Cell constants and an orientation matrix for data collection were determined by least-squares methods from the setting angles of 25 carefully centered reflections (or 23 reflections in the case of **7**·1.5CH_2Cl_2) in the range 6.73 < 2θ < 24.60° for **1**, 22.04 < 2θ < 24.58° for **2**, 22.10 <2θ < 24.42° for **3**·CH_2Cl_2, 22.05 <2θ < 24.81° for **4**·CH_2Cl_2, 22.36 < 2θ < 24.69° for **5**·2$(CH_3)_2$CHOH, 29.40 < 2θ < 31.37° for **6**·CH_2Cl_2, and 22.34 <2θ < 24.95° for **7**·1.5CH_2Cl_2. Three representative reflections were monitored at regular intervals, which showed no sign of significant decay throughout the data collection except for **7**·1.5CH_2Cl_2. In the case of **7**·1.5CH_2Cl_2, intensities of the standard reflections decreased by 44.1% over the period of data collection, probably due to the loss of the crystal solvent. An empirical absorption correction was applied by the *y* scan technique, which resulted in transmission factors ranging from 0.83 to 1.00 for **1**, from 0.71 to 1.00 for **2**, from 0.45 to 1.00 for **3**·CH_2Cl_2, from 0.58 to 1.00 for **4**·CH_2Cl_2, from 0.57 to 1.00 for **5**·2$(CH_3)_2$CHOH, from 0.55 to 1.00 for **6**·CH_2Cl_2, and from 0.70 to 1.00 for **7**·1.5CH_2Cl_2. The reflection data were also corrected for Lorentz and polarization effects.

The structures of **1**, **2**, **3**·CH_2Cl_2, **4**·CH_2Cl_2, and **6**·CH_2Cl_2 were solved by direct methods,[30] and those of **5**·2$(CH_3)_2$CHOH and **7**·1.5CH_2Cl_2 by heavy-atom Patterson methods.[31] For **1** and **2**, all of the non-hydrogen atoms were refined anisotropically. Hydrogen atoms except for those at C(1) and C(51) were put at calculated positions. W (or Mo), S(2), S(3), C(1), C(51) atoms lie in a crystallographic mirror plane, as do the P(5), F(1)−F(4), P(6), and F(6)−F(9) atoms of PF_6^- anions. In the case of **2**, some phenyl carbons were refined with comparatively high anisotropic temperature factors. For **3**·CH_2Cl_2, two phenyl rings showed signs of disorder. The phenyl ring C(45)−C(50) was found to be disordered over two nearly perpendicular orientations, and they were refined with occupancy factors of 0.5/0.5. However, we were unable to model the disorder of the other phenyl ring, C(20)−C(25), and it was refined as a rigid group. The PF_6^- anion was refined also as a rigid group. The non-hydrogen atoms, apart from the disordered phenyl carbons and PF_6^-, were refined anisotropically. Hydrogen atoms except for those at the disordered phenyl rings were included at calculated positions. In the case of **4**·CH_2Cl_2, the tungsten, copper, sulfur, phosphorus, and bromine atoms were refined anisotropically, and the carbon atoms of dppm and the solvent molecule were refined isotropically. For both **3**·CH_2Cl_2 and **4**·CH_2Cl_2, location of solvent molecules was not easy and they were refined using restrained parameters. It may be that there are more than one solvent molecules in an asymmetric unit, but we could locate only one CH_2Cl_2 for either **3** or **4**. The solvent molecule of **4**·CH_2Cl_2 is disordered and refined using restrained parameters. Being crystallized with a common acentric space group, **3** and **4** are chiral. However the absolute configuration of these molecules were not determined. For **5**·2$(CH_3)_2$CHOH, all the non-hydrogen atoms were refined anisotropically. The large anisotropic temperature factors associated with one 2-propanol solvent (O(2), C(79), C(80), C(81)) suggest slight disorder. However attempts to model this disorder failed to improve *R* values. For **6**·CH_2Cl_2, the P(6) and C(63) atoms were split into two sites with occupancy factors of 0.7/0.3. One phenyl group was also disordered over two orientations, which were refined as rigid groups with 0.7/0.3 occupancy. All the non-hydrogen atoms except for the disordered phenyl groups and the CH_2Cl_2 molecule were refined anisotropically. Crystal **7** contains 1.5 CH_2Cl_2 solvent molecules in an asymmetric unit. One CH_2Cl_2 molecule is at a general position, while the C atom of the other is situated at an inversion center and the Cl atoms are disordered with the occupancy factor of 0.5/0.5. The non-hydrogen atoms except the $[(n\text{-}Bu)_4N]^+$ carbons and two CH_2Cl_2 molecules were refined anisotropically.

The final cycle of full-matrix least-squares refinements was based on 5247 (**1**), 4969 (**2**), 6573 (**3**·CH_2Cl_2), 5573 (**4**·CH_2Cl_2), 6377 (**5**·

(30) (a) Sheldrick, G. M. SHELXS86. In *Crystallographic Computing 3*; Sheldrick, G. M., Kruger, C., Goddard, R., Eds.; Oxford University Press: Oxford, England, 1986. (b) Altomare, A.; Burla, M. C.; Camalli, M.; Cascarano, M.; Giacovazzo, C.; Guagliardi, A.; Polidori, G. SIR92. *J. Appl. Crystallogr*. **1994**, *27*, 435. (c) Beurkens, P. T.; Admiral, G.; Beurskens, G.; Bosman, W. P.; de Gelder, R.; Israel, R.; Smits, J. M. M. *DIRDIF94*: *The DIRDIF-94 program system*; Technical report of the Crystallography Laboratory; University of Nijmegen: Nijmegen, The Netherlands, 1994.

(31) Beurskens, P. T.; Admiral, G.; Beurskens, G.; Bosman, W. P.; Garcia-Granda, S.; Gould, R. O.; Smits, J. M. M.; Smykalla, C. *PATTY*: *The DIRDIF program system*; Technical Report of the Crystallography Laboratory; University of Nijmegen: Nijmegen, The Netherlands, 1992.

Table 7. Summary of Crystallographic Data for $[MS_4Cu_4(dppm)_4](PF_6)_2$ (M = W (**1**), Mo (**2**)), $[WS_4Cu_3(dppm)_3](PF_6)$ (**3**), $[WS_4Cu_3(dppm)_3]Br$ (**4**), $[Cu_3(dppm)_3Br_2]Br$ (**5**), $[WS_4Cu_2(dppm)_3]$ (**6**), and $[(n\text{-}Bu)_4N][WS_4Cu_3Br_2(dppm)_2]$ (**7**)[a]

	1	**2**	**3**·CH_2Cl_2	**4**·CH_2Cl_2	**5**·2$(CH_3)_2CHOH$	**6**·CH_2Cl_2	**7**·1.5CH_2Cl_2
formula	$C_{100}H_{88}Cu_4F_{12}P_{10}S_4W$	$C_{100}H_{88}Cu_4F_{12}MoP_{10}S_4$	$C_{76}H_{68}Cl_2Cu_3F_6P_7S_4W$	$C_{76}H_{68}BrCl_2Cu_3P_6S_4W$	$C_{81}H_{82}Br_3Cu_3O_2P_6$	$C_{76}H_{68}Cl_2Cu_2P_6S_4W$	$C_{67.5}H_{83}Br_2Cl_3Cu_3NP_4S_4W$
fw	2393.79	2305.88	1885.81	1820.75	1703.73	1677.30	1801.20
cryst syst	orthorhombic	orthorhombic	monoclinic	monoclinic	triclinic	triclinic	monoclinic
space group	*Pnma* (No. 62)	*Pnma* (No. 62)	$P2_1$ (No. 4)	$P2_1$ (No. 4)	$P\bar{1}$ (No. 2)	$P\bar{1}$ (No. 2)	$P2_1/n$ (No. 14)
a, Å	37.871(6)	38.00(3)	13.185(5)	12.94(2)	15.613(5)	14.60(3)	10.842(3)
b, Å	19.667(4)	19.65(1)	17.234(6)	17.06(1)	18.440(6)	25.6(1)	31.08(2)
c, Å	14.826(4)	14.80(1)	17.791(2)	17.875(7)	14.191(8)	10.98(1)	22.713(5)
α, deg					99.86(4)	92.9(3)	
β, deg			90.83(4)	93.7(1)	104.14(4)	105.1(1)	101.29(2)
γ, deg					86.79(3)	78.7(4)	
V, Å^3	11042(3)	11048(12)	4042(1)	3938(6)	3902(2)	3883(19)	7504(4)
Z	4	4	2	2	2	2	4
D_{calcd}, g cm^{-3}	1.440	1.386	1.549	1.535	1.450	1.434	1.594
λ(Mo Kα), Å	0.710 69	0.710 69	0.710 69	0.710 69	0.710 69	0.710 69	0.710 69
μ, cm^{-1}	20.79	11.50	25.61	31.01	25.18	23.62	37.78
R[b]	0.046	0.064	0.053	0.061	0.051	0.047	0.079
R_w[c]	0.072	0.093	0.070	0.075	0.058	0.071	0.093

[a] Crystallographic calculations were carried out with a teXsan crystallographic software package of Molecular Structure Corporation (1985 and 1992). [b] $R = \sum||F_o| - |F_c||/\sum|F_o|$. [c] $R_w = [\sum w(|F_o| - |F_c|)^2/\sum w|F_o|^2]^{1/2}$.

2$(CH_3)_2CHOH$), 10822 (**6**·CH_2Cl_2), and 5547 (**7**·1.5CH_2Cl_2) observed reflections ($I > 3.00\sigma(I)$) and 613 (**1**), 613 (**2**), 760 (**3**·CH_2Cl_2), 449 (**4**·CH_2Cl_2), 856 (**5**·2$(CH_3)_2CHOH$), 783 (**6**·CH_2Cl_2), and 671 (**7**·1.5CH_2Cl_2) variable parameters. The maximum and minimum residual peaks on the final difference Fourier map are 0.82/−0.49 (**1**), 1.42/−0.97 (**2**), 1.74/−0.94 (**3**·CH_2Cl_2), 1.36/−1.39 (**4**·CH_2Cl_2), 0.70/−0.63 (**5**·2$(CH_3)_2CHOH$), 1.69/−0.78 (**6**·CH_2Cl_2), and 1.72/−2.98 (**7**·1.5CH_2Cl_2) e/Å^3. These crystallographic data are summarized in Table 7.

Acknowledgment. J.-P.L. thanks the Japan Society for the Promotion of Science for a postdoctoral fellowship. We are grateful to Drs. Hiroyuki Kawaguchi and Michael James for discussions.

Supporting Information Available: Listings of crystallographic data, atomic coordinates and B_{iso}/B_{eq}, anisotropic displacement parameters, bond lengths and angles, structure drawings with fully labeled atomic numbering, and packing diagrams for **1**, **2**, **3**·CH_2Cl_2, **4**·CH_2Cl_2, **5**·2$(CH_3)_2CHOH$, **6**·CH_2Cl_2, and **7**·1.5CH_2Cl_2 (90 pages). Ordering information is given on any current masthead page.

IC980566C